Magnetic Resonance Elastography in Intracranial Neoplasms

A Scoping Review

Aunan-Diop, Jan Saip; Halle, Bo; Pedersen, Christian Bonde; Jensen, Ulla; Munthe, Sune; Harbo, Frederik; Andersen, Mikkel Schou; Poulsen, Frantz Rom

Published in:
Topics in magnetic resonance imaging : TMRI

DOI:
10.1097/RMR.0000000000000292

Publication date:
2022

Document version:
Final published version

OPEN

Magnetic Resonance Elastography in Intracranial Neoplasms: A Scoping Review

Jan Saip Aunan-Diop, stud. med.,[*‡] *Bo Halle, MD, PhD,*[*‡] *Christian Bonde Pedersen, MD, PhD,*[*‡] *Ulla Jensen, MSc,*[†] *Sune Munthe, MD, PhD,*[*‡] *Frederik Harbo, MD, PhD,*[†] *Mikkel Schou Andersen, MD,*[*‡] *and Frantz Rom Poulsen, MD, PhD*[*‡]

Abstract: Background: Magnetic resonance elastography (MRE) allows noninvasive assessment of intracranial tumor mechanics and may thus be predictive of intraoperative conditions. Variations in the use of technical terms complicate reading of current literature, and there is need of a review using consolidated nomenclature.

Objectives: We present an overview of current literature on MRE relating to human intracranial neoplasms using standardized nomenclature suggested by the MRE guidelines committee. We then discuss the implications of the findings, and suggest approaches for future research.

Method: We performed a systematic literature search in PubMed, Embase, and Web of Science; the articles were screened for relevance and then subjected to full text review. Technical terms were consolidated.

Results: We identified 12 studies on MRE in patients with intracranial tumors, including meningiomas, glial tumors including glioblastomas, vestibular schwannomas, hemangiopericytoma, central nervous system lymphoma, pituitary macroadenomas, and brain metastases. The studies had varying objectives that included prediction of intraoperative consistency, histological separation, prediction of adhesiveness, and exploration of the mechanobiology of tumor invasiveness and malignancy. The technical terms were translated using standardized nomenclature. The literature was highly heterogeneous in terms of image acquisition techniques, post-processing, and study design and was generally limited by small and variable cohorts.

Conclusions: MRE shows potential in predicting tumor consistency, adhesion, and mechanical homogeneity. Furthermore, MRE provides insight into malignant tumor behavior and its relation to tissue mechanics. MRE is still at a preclinical stage, but technical advances, improved understanding of soft tissue rheological impact, and larger samples are likely to enable future clinical introduction.

Key Words: elasticity, intracranial neoplasm, magnetic resonance elastography, neurosurgery, stiffness, viscoelasticity

(*Top Magn Reson Imaging* 2022;31:9–22)

From the [*]Department of Neurosurgery, Odense University Hospital, 5000 Odense, Denmark; [†]Department of Radiology, Odense University Hospital, 5000 Odense C, Denmark; and [‡]Clinical Institute, University of Southern Denmark, BRIDGE (Brain Research - Inter Disciplinary Guided Excellence), University of Southern Denmark, 5000 Odense C, Denmark.

Received for publication December 11, 2021; accepted January 13, 2022.

Address correspondence to Jan Saip Aunan-Diop, stud. med., Heden 12, 5000, Odense C, Denmark (e-mail: Jadio18@student.sdu.dk).

The study was supported by the Lundbeck Foundation through the pregraduate neurosurgical scholarship.

The authors report no conflicts of interest.

The authors hereby consent to publication according to the terms of Neurosurgical Review. Patient consent not applicable.

DOI: 10.1097/RMR.0000000000000292

Magnetic resonance elastography (MRE) is a novel imaging modality that allows quantitative assessments of tissue mechanics. The technique is often described as the radiological equivalent of palpation as its major application is noninvasive evaluation of tissue consistency. MRE studies on intracranial neoplasms are of great interest in clinical neurosurgery. However, interpretation and data comparison are complicated by the technical nature of MRE, inconsistent use of nomenclature, and wide range of study designs as well as incoherent cohorts.

The MRE Guidelines Committee has recently published a set of guidelines in a collaborative effort across researchers to address these issues.[1] In view of the heterogeneity of MRE studies, we use these guidelines as a framework for the present review to maximize accuracy, consistency, and readability. Our aim is to present a structured overview of current MRE literature on intracranial neoplasm in humans. We identify trends, differences, and challenges in the current brain MRE literature and suggest approaches for improving study reproducibility and data quality.

INTRACRANIAL NEOPLASMS

Modern neurosurgery is a highly technical field where neuroimaging plays a central role. The integration of neuroradiological methods has greatly improved diagnostic and treatment options in neuro-oncological surgery. Tumor consistency, adhesions, and structural homogeneity are important variables which influence tumor resectability. For example, hard adherent tumors may require the use of ultrasonic aspiration at high setting, extended operating time, and prolonged manipulation in the tumor-brain interface. Thus, the risk of complications is altered. Brain MRE provides information related to these parameters preoperatively and noninvasively. Multiple attempts to describe these parameters by conventional magnetic resonance imaging (MRI) have had very limited success,[2] and in most cases the information is first available to the surgeon during surgery. Presurgical prediction of intraoperative conditions could be beneficial for preoperative planning and surgical risk stratification. Access to elastographic data before surgery could help to orientate the surgical field and improve resection and on-site decision making. The consistency of meningiomas can range from a soft tumor that is removable by suction to a hard mass that require piecemeal removal and ultrasonic aspiration.[3] Meningiomas that are adherent to surrounding tissue require careful and strenuous advancement in the resection plane. Similar challenges are encountered in schwannomas and pituitary adenomas and complicate their removal from deep cranial sites,[4,5] often using minimally invasive endoscopic approaches.

MRE parameters provide unique insight into the in vivo mechanical properties of tissue and contribute to our understanding of the biomechanical conditions, which seem to be closely related to tumor biology and behavior. For example extracellular matrix (ECM) stiffness has been related to malignant attributes in glioblastomas,[6] and MRE studies on breast tumors found that tumor stiffness increased with increasing tumor grade.[7] Although T1-, T2-, and

gadolinium-enhanced MRI sequences are cornerstones in clinical diagnosis and in monitoring of glial tumors,[8] they lack biological specificity. Furthermore, gadolinium enhancement requires increased blood-brain barrier permeability, which may be absent at an early tumor stage.[8] MRE measures mechanical properties that vary by more than five orders of magnitude in different tissues[9] and may thus contribute valuable supplementary information in a paraclinical setting. For example, MRE may have a role in early detection of tumors, and in evaluating the peritumoral tissue invasion and guide the need for aggressive resection.

BRIEF TECHNICAL BACKGROUND

MRE is a phase contrast-based MRI technique that depicts the spread of mechanical waves in tissues. The acquired data can be used to display several aspects of tissue mechanics such as elastic and viscoelastic behavior, and tissue damping properties. The acquired parameters are related to haptic properties such as tissue consistency that can be evaluated by touch.

Simplified MRE can be described in three stages.[9–11] First, stress is introduced by mechanical waves that cause tissue excitation (i.e., deformation). Second, image acquisition uses phase contrast MRI sequences to record the propagation of the waves in tissues. Third, inversion involves a series of complex mathematical operations that extract information about tissue properties (Fig. 1).

Mechanical excitation introduces shear waves and longitudinal waves to the tissues. Longitudinal waves propagate at high speeds at common driving frequencies and are a source of noise. Effort is often taken to reduce this effect, for example, by filtering or taking the curl of the displacement field. Shear waves propagate at varying speeds of approx. 1 to 5 m/s in different tissues and cause compression in the magnitude of tens of microns.[1] It is this variation that forms the basis for MRE acquisition.[1] The common approach to excitation is use of an external wave generator that typically consists of a wave-generating component, that is, active driver, and a passive driver component that is responsible for conduction of the waves to the skull and the brain.[12] Generators use air pressure, sound, piezoelectric, or rotational mechanical components to produce waves at specific frequencies. Harmonic excitation at a single frequency is common, typically around 60 Hz. Excitation at multiple frequencies, known as multi frequency MRE (MMRE), is sometimes employed. Vibration frequencies and wave amplitude have a direct effect on measured values.[1] This can be explained by the viscoelastic behavior of soft tissues. While purely elastic bodies have a linear stress/strain relationship, viscoelastic bodies display a nonlinear response.[13] Soft tissues thus become stiffer as loading increases,[13] a behavior that can be probed in MMRE. Furthermore, vibration frequencies affect the signal-to-noise ratio (SNR), wave attenuation, and penetration depth[12] as viscous tissue behavior dampens the waves (i.e., energy loss).

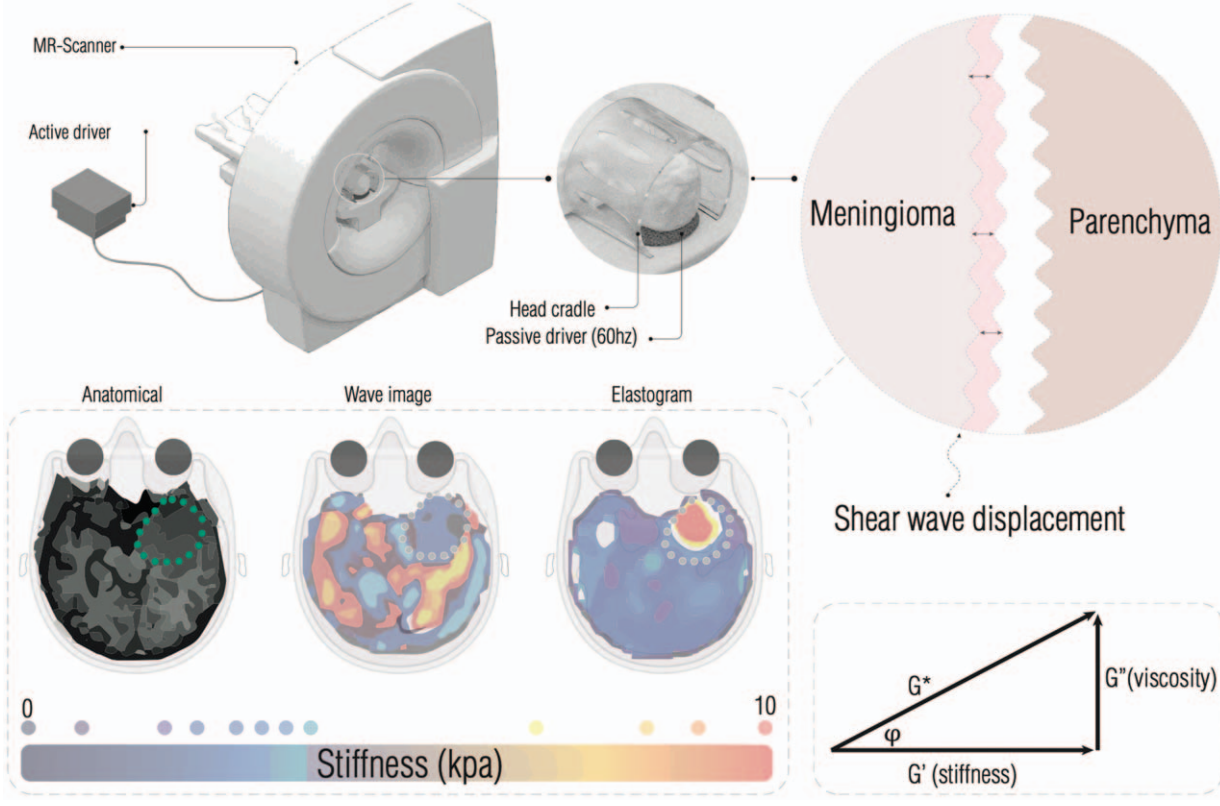

FIGURE 1. Overview of MRE technique: the active driver generates mechanical waves which are transferred to the skull via the passive driver component. The mechanical waves cause oscillations and displacement of soft tissues. Multiple phase contrast images are obtained at different time points in the displacement cycles. The displacement data is used to generate wave images where each pixel is described by local displacement in time. Elastograms may then be generated by inversion. These ''stiffness'' maps obtain contrast by the ''stiffness'' value in each pixel, typically by G^* or G'. Similarly, viscosity maps can be generated by considering the loss of energy in the mechanical waves, that is, damping G'' or φ. MRE, magnetic resonance elastography.

TABLE 1. Technical Terminology

Elasticity, viscosity, viscoelasticity	Elasticity is the property of a body to return to its original shape. Viscosity is the strain rate of a body (i.e., how fast deformation occurs when stress is applied). Soft tissues display both properties and are therefore viscoelastic.
Stiffness	In MRE studies, stiffness is often used as a comparative term, usually when comparing shear moduli, shear stiffness, shear modulus magnitude, etc.
Viscosity	Describes a fluid's resistance to flow. In viscous bodies, there is a time lag between the applied stress and strain response—in contrast to bodies with low viscosity (high fluidity). The loss modulus, damping ratio, shear modulus phase angle, and loss tangent are related to the viscosity of tissues.
Fourier transformation	A mathematical operation that reduce a time-dependent function to a frequency-dependent function. The transformation is used to extract motion at the driving frequency, a complex number in each pixel that consists of the wave amplitude and phase.
Helmholtz equation $G^* = pw^2/\Delta^2 u$ p is the density w is the angular frequency u is the complex harmonic displacement (vector or curl)	Used for extracting $G*$ from the complex harmonic displacement data. Assumes local homogenicity (i.e., material has same properties in all directions). It is sensitive to noise, and the effect of long wave lengths should be reduced by filtering or using the curl of the wave field.
Shear stiffness (U) $U = pc^2$ p is the density c is the wave speed	Described as an effective shear modulus of an elastic material that exhibits a particular wave speed at a specific driving frequency. Shear stiffness is closely related to $\|G*\|$, $G*$, G', and G''. The wave speed is often derived using an inversion method called local frequency estimation, and tissue density is assumed to be that of water.
Shear modulus (G or u)	Relative stiffness measure when the material is assumed to be purely elastic (does not dissipate energy). The stress-strain relationship is linear, and the shear modulus is the slope of this function.
Complex shear modulus ($G*$) $G* = G' + iG''$ G' is the storage modulus i is an imaginary number G'' is the loss modulus	The shear modulus of soft tissues is expressed by a complex quantity because viscoelastic bodies display a nonlinear stress-strain relationship. In MRE, the value depends on the driving frequency. $G*$ is the slope of the tangent at a specific frequency in a stress/strain curve. When $G*$ is extracted using the Helmholtz equation, the equation for $G*$ can be solved as $G* = G' + iG''$ thus providing the storage- and loss moduli.
Storage modulus (G')	Measures stored energy at the applied wave frequency and is related to the elastic component of $G*$
Loss modulus (G'')	Measures the loss of energy in a wave and is related to the viscous component of $G*$.
Shear modulus magnitude $\|G*\|$	Quantifies the total size of storage and loss properties and is expected to increase when the density of tissue network structure increases. $G*$ is extracted using the Helmholtz equation The equation for the complex shear modulus can be solved as $G* = \|G*\|(\cos\varphi + i\sin\varphi)$ thus providing the complex shear modulus and the shear modulus phase angle.
Shear modulus phase angle (φ) $\varphi = (\arctan[G''/G'])$	Describes a lag phase between stress and strain. For pure elastic material, this angle is 0°; for purely viscous materials, the angle is 90°. The shear modulus phase angle describes dissipative behavior in tissues and the degree to which the value of $G*$ can be assigned to viscous or elastic components.

MRE indicates magnetic resonance elastography.

Image acquisition uses motion encoding gradients (MEG) to encode displacement into the MR phase signal.[10,14] Acquisitions are typically acquired in three directions (x, y, z) to derive the three-dimensional displacement vector, represented by the signal at each pixel.[1,12] Often, multiple acquisitions are made during a phase (phase offsets), and a Fourier transformation (Table 1) is used to extract the motion at the driving frequency. This motion is described by a complex number at each pixel that contains the wave amplitude and phase.[1,12] The images containing information about displacement in time are referred to as wave images.

Inversion is the process of extracting material properties from wave images. Many inversion algorithms are based on the Helmholtz equation (Table 1)[1] that is used to extract the complex shear modulus ($G*$) from the motion at the driving frequency. The shear modulus can be expressed as a complex quantity because energy is lost as the wave propagates. The complex shear modulus ($G*$) has an elastic part, termed the storage modulus (G'), and a viscous part called the loss modulus (G''). Alternatively, the wave field can be described directly. Some studies use viscoelastic models to further describe nonlinear viscoelastic behavior at different driving frequencies. Table 1 presents an overview of relevant parameters and technical terms used in this review.

METHODS

Protocol

The protocol was based on PRISMA Extension for Scoping Reviews (PRISMA-ScR).[15]

Eligibility Criteria

Peer-reviewed journal papers published in English were included. Eligible studies were those that acquired brain MRE on patients with intracranial neoplasms. Only human studies with experimental or quasi-experimental designs were included.

Exclusion criteria were animal studies, review articles, or systematic reviews, and conference abstracts.

Search Strategy

The search string was built by extracting key terms from relevant articles acquired by free searching and from known literature. Key terms were collected in a table and rated according to frequency. From this, a general search string was constructed and

tested. The search string was refined and then modified for each database using, for example, the MESH database vocabulary look-up aid. Databases included were PubMed (Medline, PubMed central), Embase, and Web of Science. The final search in all databases was performed on February 14, 2021. The result of each search was exported to *Endnote x9.3.3*. The time of the search and the search string were documented for each database.

As an example, the search string from PubMed was:

((''elasticity imaging techniques''[MeSH Terms] OR ''MRE''[All Fields] OR ''magnetic resonance elastography''[All Fields] OR ''MR elastography''[All Fields] OR ''slip interface''[All Fields]) AND (''brain''[MeSH Terms] OR ''brain''[All Fields] OR ''brains''[All Fields] OR ''brain s''[All Fields])) NOT ''animal''[Title/Abstract]

Selection of Sources and Data items

Each title and abstract was screened by the first author (JSA-D) for relevance. When in doubt, a senior author (FRP) was asked for a second opinion and the issue was resolved through discussion. The articles that passed the title/abstract screening went through a full-text review and were categorized as either included, excluded, or undecided by the first author. All undecided articles went through a second full-text review. The articles were simultaneously screened for inclusion in another review of MRE studies on normal pressure hydrocephalus. Figure 1 presents an overview of the search and selection process.

Data items are represented in Table 2. They included tumor histology and number, field strength (Tesla), MRI scanner type, excitation source, excitation frequency (Hz), wave generation strategy, MRI sequence, regions of interest (ROIs), and main results.

RESULTS

Twelve articles were included in the review and are presented in Figure 2.

Studies on Brain Tumor Consistency

Studies Comparing Tumors with Different Histology

Multiple attempts have been made to predict the consistency of brain tumors using MRE. The earliest study identified in our search was made by Xu et al[16] in 2007. This preliminary study assessed tumor consistency through preoperative MRE and intraoperative grading of tumor consistency. The study included six patients with known solid brain tumors: four meningiomas (MEN), one vestibular schwannoma (VS), and one hemangiopericytoma. Single frequency (150 Hz) MRE was made prior to tumor resection, and the axial section with the highest tumor diameter was used. ROIs are described in Table 2. Local frequency estimated wavelengths (c) were extracted for each ROI. The wavelengths were classified as shorter, longer, or similar relative to the wavelength of the white matter. Shear stiffness (U) was calculated from the wavelengths, assuming tissue density to be equal to that of water.[17] U_{tumor} was compared to that of normal-appearing white matter (NAWM). Perioperatively, the tumors were rated qualitatively as soft, intermediate, or hard by a single rater blinded to the MRE result. The authors observed that both the wavelength and the U agreed with the intraoperative assessment in all six cases. The softer tumors had shorter wavelengths and lower U compared to NAWM. In contrast, harder tumors had longer wavelengths and higher U relative to NAWM. The study is limited by single slice analysis and does not report quantitative data. It should be regarded as a pioneering effort in applying MRE to evaluate the consistency of intracranial neoplasms.

Simon et al[18] used MRE to explore viscoelasticity in relation to malignancy. Sixteen patients with suspected intracranial malignancy were included (Table 2). The patients underwent single frequency 3DMRE (45 Hz), and the tumor ROIs were generated by delineating tumor volume on T2-weighted images manually. A reference ROI with NAWM was defined in a corresponding area in the contralateral hemisphere. The complex shear modulus was extracted by applying the Helmholtz equation to the curl of the wave field. Results were reported as the mean shear modulus magnitude ($|G*|$) and shear modulus phase angle (φ) for each ROI. Ratios of tumor and NAWM were calculated ($|G*|_{\text{tumor}}/|G*|_{\text{NAWM}}$ and $\varphi_{\text{tumor}}/\varphi_{\text{NAWM}}$) to reduce the effect of age and gender.[19] The tumor material collected for histological evaluation was described according to WHO type criteria. The $|G*|$of the tumor tissue had a range from 0.89 to 2.131 kPa. A glioblastoma (GBM) was reported to have the lowest value, and a WHO grade I MEN had the highest value. A colonic adenocarcinoma metastasis and a primary B-cell lymphoma had comparable $|G*|$ values to that of NAWM. Both meningiomas were stiffer than the NAWM (i.e., 30% and 39% higher). The seven WHO grade II–III tumors were in general softer than that of NAWM (10.9–42.3% softer). φ ranged from 0.207 to 0.749, where the highest value was found in a MEN, and the lowest value was found in a bronchial adenocarcinoma. MENs were the only tumors that had $\varphi_{\text{tumor}}/\varphi_{\text{NAWM}}$ above 1, which was in contrast to the malignant tumors.

The study suggests that malignant behavior is linked to tumor stiffness and damping properties relative to the parenchyma.

Sakai et al[20] measured stiffness in four different intracranial tumors and assessed the potential of MRE to detect firm tumors. The study included 34 patients scheduled for tumor resection (Table 2). Prior to surgery, patients underwent single frequency MRE (40 Hz). ROIs corresponding to the tumors were manually defined on wave images based on conventional MRI, contrast-, and diffusion-weighted images. Areas with interference and significant noise were excluded. Tumor stiffness was reported as the mean and max shear stiffness (U and U_{max}). Perioperative grading of tumor consistency was based on a 5-point scale where tumors with a score of 4 to 5 were considered to be ''firm'', and the remaining tumors were considered ''non-firm''. Tumor biopsies were subject to pathohistological examination and classified accordingly. MENs (mean U 1.9 ± 0.8 kPa and U_{max} 3.4 ± 1.5 kPa) were significantly stiffer than pituitary macroadenomas (PMA) (U 1.2 ± 0.3 kPa and U_{max} 1.8 ± 0.5 kPa) ($P < 0.05$). Intraoperative consistency correlated significantly with the G'_{max} of the MENs ($P = 0.04$). The mean U and U_{max} of the remaining groups of tumors (glial tumors and VS) correlated significantly with intraoperative grading ($P < 0.05$). Five tumors were grouped as firm (mean U 3.0 ± 2.6 kPa and G'_{max} 4.2 ± 1.9 kPa), and the other 29 tumors were grouped as non-firm (mean U 1.6 ± 2.6 kPa and U_{max} 2.4 ± 1.2 kPa). U_{max} was significantly higher in the firm group ($P < 0.05$). The study suggests that MRE may have a role in the preoperative detection of firm tumors. Overlapping shear stiffness values rendered histological discrimination implausible.

Reiss-Zimmerman et al[21] compared viscoelastic and damping properties in cerebral masses using 3DMMRE. The study included 27 patients: GBM (n = 11), anaplastic astrocytomas (AA; n = 3), MEN (n = 7), metastases (n = 5), and abscess (n = 1) (Table 2). All subjects underwent MMRE (30–60 Hz) after preoperative staging and workup. A Gaussian filter was applied to reduce the effect of longitudinal waves. Motion at the driving frequencies was extracted with a Fourier transformation, and the curl of the data was derived. Elastograms were generated with a multi-frequency dual elasto-visco (MDEV) inversion algorithm[22] that involved averaging the pattern of waves and the Laplace operators across frequency, prior to acquisition of tissue property parameters. ROIs for high grade tumors were defined according to the blood-brain barrier (BBB) breakdown on

TABLE 2. Overview of Current Literature

Authors, Year	Histology (n)	Field Strength (Scanner Type), Excitation Source (Frequency in Hz), Wave Generation	Sequence	ROIs	Main Results
Xu et al 2007	MEN (n = 4) VS (n = 1) HPC (n = 1)	1.5 T (Sonata, Siemens), head plate/bite plate (150 Hz), electromechanical	Phase contrast gradient echo	Tumor NAWM	Wavelength and shear stiffness (U) of tumor relative to NAWM agreed with intraoperative consistency.
Simon et al 2013	GBM (n = 3) WHO II glioma (n = 5) WHO III anaplastic glioma (n = 2) MEN (n = 2) Primary CNS lymphoma (n = 1) Metastases (n = 3)	3.0 T (GE), head cradle (45 Hz), acoustic	EPI	Tumor NAWM	Compared tumor $\|G*\|$ and φ to NAWM. $\|G*\|_{tumor}$ range was 0.89–2.131 kPa. GBM was softest. WHO II and III gliomas were generally softer than NAWM. MEN were stiffer than NAWM and had the highest φ values.
Sakai et al 2016	PMA (n = 11) VS (n = 6) WHO III glioma (n = 3) GBM (n = 3) MEN (n = 13)	3.0 T (Philips, Achieva), pillow-like (40 Hz), pneumatic	Spin echo EPI	Tumor	Compared mean U and U_{max} with intraoperative consistency. MEN were significantly stiffer than PMA. MEN U_{max} correlated with intraoperative grading Mean U and U_{max} of PMA, VS, GBM/glioma correlated with intraoperative grading. Firm tumors had significantly higher U_{max} than nonfirm tumors.
Reiss-Zimmerman et al 2015	GBM (n = 11) AA (n = 3) MEN (n = 7) Metastases (n = 5) Abscess (n = 1)	3.0 T (GE), head-cradle (30–60 Hz), acoustic	Spin echo EPI	Tumor NAWM	Compared $\|G*\|$ and φ to NAWM High grade tumors were generally softer than low grade tumors. Inverse relationship between φ and tumor grade. MEN had $\varphi_{tumor}/\varphi_{NAWM}$ above 1, all other tumors below 1.
Murphy et al 2013	MEN (n = 12)	1.5 T (Sonata, Siemens), pillow-like (60 Hz), pneumatic	Spin echo EPI	Tumor Peritumoral	Compared G' and $G'_{tumor}/G'_{peritumor}$ with intraoperative consistency. Both reached significance.
Hughes et al 2015	MEN (n = 15)	3.0 T (Signa Excite, GE), pillow-like (60 Hz), pneumatic	Spin echo EPI	Tumor	Compared mean G' of tumor correlated significantly with intraoperative consistency. MRE had good PPV and specificity in detecting intraoperative consistency, homo-, and heterogeneity.
Streitberger et al 2014	GBM (n = 22)	1.5 T (Magnetom Sonata, Siemens), head-cradle (30–60 Hz), piezoelectric 3.0 T (Trio, Siemens), head-cradle (30–60 Hz), piezoelectric	Spin echo EPI	Tumor Peritumoral edema Homogenous appearing matter (HAM) Perifocal NAWM	GBM were generally softer and more elastic than brain parenchyma. GBM had significantly lower mean $\|G*\|$ (5/22 cases) and mean φ (22/22 cases) than NAWM. HAM had mean $\|G*\|$ comparable to NAWM and mean φ lower than NAWM. HAM had higher mean $\|G*\|$ than tumor but comparable mean φ. Peritumoral edema had higher mean $\|G*\|$ than tumor. The perifocal region had significantly increased φ than NAWM.

TABLE 2. (*Continued*)

Authors, Year	Histology (n)	Field Strength (Scanner Type), Excitation Source (Frequency in Hz), Wave Generation	Sequence	ROIs	Main Results
Pepin et al 2018	WHO II gliomas (n = 5) WHO III gliomas (n = 7) WHO IV GBM (n = 6) 12 of these where IDH1 mutated and 6 IDH1 wildtype	3.0 T (Signa Excite, GE), pillow-like (60 Hz), acoustic	Spin echo EPI	Tumor NAWM	Gliomas had significantly lower $\|G*\|$ than NAWM. WHO IV GBM had significantly lower $\|G*\|$ than WHO II gliomas; no other groups could be distinguished. IDH1 wild type had significantly lower $\|G*\|$ than IDH1 mutated tumors and were therefore softer.
Streitberger et al 2020	GBM (n = 9) MEN (n = 9)	3.0 T (Magnetom Trio, Siemens), head-cradle (30–60 Hz), piezoelectric	Spin echo EPI	Tumor NAWM	GBM had lower mean $\|G*\|$ and φ than NAWM and behaved similar to soft elastic bodies. MEN had lower $\|G*\|$ and higher φ than NAWM and were fluid with higher viscosity than the parenchyma.
Hughes et al 2016	PMA (n = 10)	3.0 T (GE), pillow-like (60 Hz), pneumatic	Spin echo EPI	Tumor	Separated mean G' separated soft and intermediate intraoperative consistencies.
Yin et al 2015	VS (n = 9)	3.0 T (Signa Excite, GE), pillow-like (60 Hz), acoustic	Spin echo EPI	Shear lines and OSS values were detected	Good agreement between perioperative and SII predicted adhesion. OSS decreased with increasing perioperative adhesion
Yin et al 2016	MEN (n = 25)	3.0 T (Signa Excite, GE), pillow-like (60 Hz), acoustic	Spin echo EPI	Shear lines and OSS values were detected	Fair agreement between surgical resection plane and OSS/shear line maps. Good agreement between surgical resection plane and normalized OSS maps. OSS, shear line, and normalized OSS maps correlated significantly with surgical resection plane.

AA indicates anaplastic astrocytoma; CNS, central nervous system; EPI, echo planar imaging; G', storage modulus; $|G*|$, magnitude of the complex shear modulus; GBM, glioblastoma multiforme; HPC, hemangiopericytoma; Hz, Hertz; IDH, isocitrate dehydrogenase; MEN, meningioma; n, number; NAWM, normal-appearing white matter; OSS, octahedral shear strain; PMA; pituitary macroadenoma; PPV, positive predictive value; ROI, region of interest; SII, slip interface imaging; T, Tesla; VS, vestibular schwannoma; φ, shear modulus phase angle.

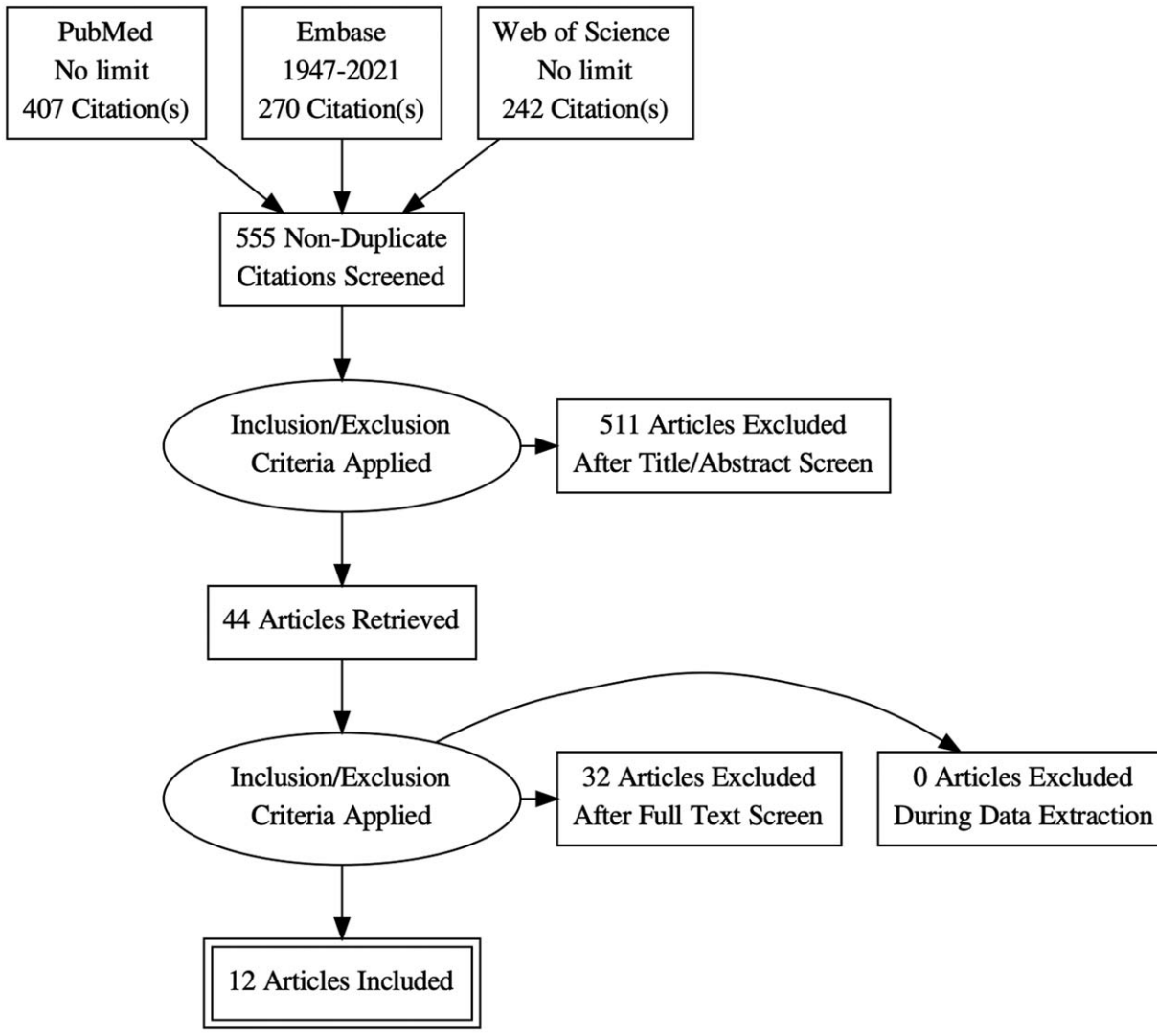

FIGURE 2. Search, screening, and selection.

contrast-enhanced T1s. For low grade tumors, local T2 signal alterations defined the ROI border. A reference NAWM was defined in the contralateral hemisphere. Results were reported as mean of the shear modulus magnitude ($|G*|$) and shear modulus phase angle (φ) for each ROI. Ratios of tumor and NAWM were calculated as ($|G*|_{\text{tumor}}/|G*|_{\text{NAWM}}$) and ($\varphi_{\text{tumor}}/\varphi_{\text{NAWM}}$).

The tumors had a $|G*|$ range from 0.87 kPa to 1.95 kPa. Generally, high grade tumors had lower $|G*|$ than low grade tumors. $|G*|$ was not able to discriminate the histological tumor type due to overlapping values. φ generally decreased with increasing WHO grade. Meningiomas were the only tumors that had $\varphi_{\text{tumor}}/\varphi_{\text{NAWM}}$ above 1.

The results indicate that malignant behavior is linked to soft elastic tumor properties. Low grade tumors are stiffer and have φ values within the range of fluids (i.e., $>90^\circ$). The incompressibility of fluid components may contribute to hard tumor consistency at high strain rates (i.e., palpation), while at low strain rates the fluid may have time to displace.[13]

Studies on Meningioma Consistency

Murphy et al[23] used MRE to predict intraoperative MEN consistency. Twelve tumors were included in the final study, and single frequency MRE (60 Hz) was acquired prior to tumor resection. Phase difference images were generated from the product of positive and negative motions, for each MEG direction. A direct inversion algorithm was applied to derive tissue properties from the curl of the data[24] after filtering. Two ROIs were defined by manual tracking on T1 images corresponding to the tumor to the peritumoral region. Prior to this, a brain mask was applied to the T1s to remove voxels with significant cerebrospinal fluid (CSF) contribution. The regions with the masks were then transferred to the MRE data. The edges of the tumor were masked to reduce the edge bias. The median storage modulus (G') of the ROIs were reported. Intraoperative grading was based on a reproducible 5-point scale, where 5 described the stiffest tumors.[3] MRE measured stiffness correlated significantly with the surgeons' assessment ($P = 0.023$). A plot of the two variables indicated an overlap in data points across categories but with an

increasing trend in G' as the stiffness categories increased. A ratio ($G'_{tumor}/G'_{peritumor}$) was calculated. The ratio was assessed for correlation with the qualitative consistency and improved significance ($P = 0.0032$). The study indicates that MRE has a possible application in preoperative assessment of meningioma consistency.

Hughes et al[25] applied a higher resolution MRE technique than Murphy et al[23] in their study on meningioma consistency and mechanical heterogenicity. The resolution in MRE describes elastographic details rather than pixel, but accurate assessments of resolution remains challenging.[1] MRE (60 Hz) was performed in 14 intracranial meningioma patients prior to surgery, allowing data collection from 15 tumors. Post-processing was identical to that reported by Murphy et al,[23] except that images were acquired with higher repetition time (TR), slice number, and phase offsets. Stiffness was reported as the median storage modulus (G') of the tumor ROIs. Tumors with mean $G' > 6$ kPa were considered to be hard (range 0–8 kPa). Tumors were described as heterogeneous if approximately 20% of the G' values appeared to be of distinctly different quantities. If resection generally required interchangeable instrument use, the tumor was classed as heterogeneous. Approximate descriptions of hologenetic locations were made. Intraoperative evaluation of consistency was made according to a 5-point scale.[3] The vascularity of the tumor was also assessed. Durometric measures of surgical specimen yielded semi-quantitative comparative consistency values. The surgeons described eight tumors as heterogeneous, of which five were described as heterogeneous on MREs (62.5% agreement). Of the seven tumors described intraoperatively as homogenous, five were assessed to be homogenous on MRE (71.4% agreement). Notably, four out of four soft homogenous tumors were described identically (100% agreement). The correlation between surgical grading and MRE-measured consistency reached significance ($P = 0.02$). Correlations between mean G' and durometer measurements, then durometer measurements and surgical grading were significant ($P = 0.03$ and $P = 0.01$, respectively). The positive predictive value (PPV) and specificity for detecting hard and heterogeneous tumors were 100%. In predicting homogeneity, MRE had a specificity of 78% and a PPV of 75%. In predicting a soft consistency, PPV was 86% but specificity was only 33%. MRE had 60% specificity in ruling out hardness. The authors reported that tumor size $\leq$3.5 cm and high tumor vascularity were associated with lower correlation between MRE-measured and surgically graded consistency ($P < 0.05$). The study is strongly suggestive of a possible clinical application of MRE in predicting meningioma consistency and mechanical heterogeneity.

Studies on Gliomas and Glioblastoma Consistency

Streitberger et al[26] studied glioblastomas and their relation to surrounding tissue. The study included 22 patients with GBMs. Prior to planned procedures, the patients underwent MMRE (20–60 Hz). Two different MRE scanners were used in the trial, and 11 patients were scanned using each device. Image acquisition parameters differed (Table 2) due to different scanner field strengths (1.5 T vs. 3.0 T). Post-processing MDEV inversion was applied.[22] ROIs corresponding to the tumor, peritumoral edema, and NAWM were traced manually. An ROI within the tumor with homogenous-appearing matter (HAM) was defined. A perifocal ROI was defined by increasing the tumor ROI by 3 pixels, then subtracting the tumor volume. Conventional MRI (T1, T2, and contrast-enhanced) were used to assess and grade tumor morphology (necrosis, cyst, hemorrhages, homogeneity, etc.).

MRE results were presented as the shear modulus magnitude ($|G*|$) and shear modulus phase angle (φ) for each ROI. The mean $|G*|$ of the GBMs was 1.32 ± 0.26 kPa (range 0.85–1.83 kPa). Glioblastoma tissue was significantly softer than NAWM (mean $|G*|$ 1.54 ± 0.27 kPa, $P = 0.001$). Five GBMs were stiffer than NAWM. The φ was significantly lower in GBM (mean $\varphi_{tumor} = 0.37 \pm 0.08°$) than in the NAWM (mean $\varphi_{NAWM} = 0.58 \pm 0.07°$) in all 22 tumors ($P = 2.9 \times 10^{-10}$).

HAM had higher $|G*|$ compared to the whole tumor ($P < 0.05$) and was not significantly different from NAWM. Mean φ in the HAM was significantly lower than that of healthy tissue ($P = 0.04$) but not significantly different from that of the whole tumor. In perifocal ROIs, mean $|G*|$ did not significantly differ from that of the tumor, however φ increased significantly ($P = 0.001$). Peritumoral edema was stiffer than tumor tissue ($P = 0.004$), but the phase angle was not significantly different. There were no significant correlations in morphology assessed on MRI- and MRE-derived parameters. When comparing the data between the two different scanners, only $|G*|_{NAWM}$ differed significantly ($P = 0.001$). Generally, GBMs were found to be softer and more elastic than normal parenchyma (Table 1). The study suggests that glioblastomas behave similarly to soft elastic bodies.

Pepin et al[27] linked viscoelasticity to *isocitrate dehydrogenase 1 (IDH1)* status in their study on glial tumors. IDH1 is an important prognostic marker where the *IDH1 wild type* is associated with poorer prognosis and more aggressive tumor behavior. Eighteen patients with biopsy-confirmed gliomas (WHO II n = 5, WHO III n = 7, WHO IV n = 6) were included; 12 of these tumors had IDH1-R132 mutations. Prior to resection, patients underwent single frequency MRE (60 Hz). Complex phase difference images were generated. The data were filtered and inverted based on the curl of the wave field data. MRE results were reported as the mean magnitude of the complex shear modulus ($|G*|$). Tumor and NAWM ROIs were defined. After the surgical procedure, the tumors were categorized according to tumor grade, histological subtype, 1p/19q co-deletion, and IDH1-R132H status.

Mean $|G*|_{tumor}$ was 2.2 ± 0.7 kPa (1.1–3.8 kPa) and mean $|G*|_{NAWM}$ was 3.3 ± 0.7 kPa (1.2–4.1 kPa). The tumors were significantly softer than NAWM ($P < 0.001$). In general, high-grade gliomas were softer than low-grade gliomas, indicating an inverse relationship between tumor grade and $|G*|$. Grade IV GBMs (1.7 ± 0.5 kPa, range 1.3–2.1 kPa) were significantly softer than grade II gliomas (2.7 ± 0.7 kPa, range 1.3–2.1 kPa) ($P = 0.03$) but could not be separated from grade III gliomas. There were no significant differences between grade III and IV, or between grade II and III. Gliomas with IDH1 mutations (2.5 ± 0.6 kPa, range 1.5–3.8 kPa) were stiffer than wild type tumors (1.6 ± 0.3 kPa, range 1.1–1.9 kPa) independent of tumor grade ($P = 0.007$). The study indicates that gliomas are softer than healthy parenchyma, $|G*|$ decreases with increasing WHO grade, and *wild type* gliomas appear to be softer. Thus, malignant potential was again linked to glioma consistency.

Streitberger et al[28] also explored the relationships between tumor viscosity, elasticity, and malignancy. The study consisted of two parts. In the first part, three phantom materials (heparin, water, agar-water, and tofu-water) were blended in different water to-gel/solid fractions to assess the effect on MRE measured fluidity/viscosity with increasing water content. In the second part, fluidity, stiffness, and water content of GBMs and MENs were assessed.

The study included 18 patients (GBM n = 9, WHO I MEN n = 9). MMRE (30–60 Hz) and conventional MRI (T1, T2) were obtained. Post-processing steps were similar to Streitberger et al.[26] MDEV inversion[22] was used to acquire $|G*|$ and φ for ROIs corresponding to the tumor and NAWM. Relative water content in the tumor was measured using the magnitude of the complex MRI signal ($|S*|$). The phantoms were imaged in cylindrical containers using the same MMRE and inversion technique.

All phantoms showed a decrease in $|G*|$ with increasing water content. φ values were unchanged in heparin, increased with dilution

in agar, and decreased with dilution in tofu. Thus, φ reflects material properties that are distinctly different from $|G*|$. The mean $|G*|_{MEN}$ (1.51 ± 0.34 kPa) and the mean $|G*|_{GBM}$ (1.10 ± 0.29 kPa) were significantly lower than the references $|G*|_{NAWM}$ (1.78 ± 0.25 kPa, $P = 0.009$, and 1.81 ± 0.23 kPa, $P < 0.001$). φ_{GBM} ($0.36 \pm 0.10^{\circ}$) was significantly lower than φ_{NAWM} ($0.65 \pm 0.04^{\circ}$) ($P < 10^{-4}$). The φ_{MEN} ($1.0 \pm 0.13^{\circ}$) was significantly higher than the reference φ_{NAWM} ($0.58 \pm 0.07^{\circ}$) ($P < 10^{-4}$). $|S*|$ suggested higher water content in GBMs and lower water contents in MENs. There was an inverse relationship between tumor water content ($|S*|$) and φ ($P < 0.001$). This behavior was also found in the tofu phantom. The study suggests that glioblastomas can be described as very soft solids with lower viscosity than parenchyma. Meningiomas can be described as fluids with viscosity higher than surrounding tissue. The difference may be related to the natural high glycosaminoglycan (GAG) content of glial tumors. The observation supports a viscous fingering theory of invasive growth[29,30] where a fluid of lower viscosity may spread in with a fluid with higher viscosity due to interface instability.

Studies on Pituitary Adenoma Consistency

Hughes et al[4] assessed the ability of MRE to describe the consistency of PMAs. The study included 10 patients with PMAs that were subjected to single frequency MRE (60 Hz) prior to transsphenoidal resection. Median storage modulus (G') was reported for each tumor ROI. Tumor consistency was assessed perioperatively, and the tumors were described as soft, intermediate, or hard based on suckability and sharp resection requirements. Six tumors were described as soft, and four as intermediate.

The soft tumors had a mean G' of 1.38 ± 0.36 kPa (1.08–1.86 kPa). Intermediate tumors had a mean $G' = 1.94 \pm 0.26$ (1.72–2.32). The groups were significantly different ($P = 0.020$).

The study indicates that MRE may be useful in predicting the consistency of PMAs.

Studies on Brain Tumor Adhesion

Two studies by Yin et al applied slip interface imaging (SII) to predict tumor-brain adhesion. The method is based on detection of a gliding interface at tissues borders, caused by a difference in motion, scattering, etc. across the slit. In the absence of gliding interfaces, the tumor can be considered adhesive to the surrounding tissue (i.e., motion spreads easily across the interface). Octahedral shear strain (OSS) represents the maximum pixel displacement in any direction, and high OSS values at the interface are indicative of low resistance to movement. Intra voxel phase dispersion (IVPD) is caused by a phase shift (in waves) due to large differential motion across a surface[31] and are visible as shear lines. The first study[5] included nine patients with VS. Single frequency MRE (60 Hz) was obtained prior to surgery and processed to generate slip interface images. OSS values and the presence of low-intensity shear lines were used to describe the slip interface as (1) complete, (2) partially adhesive, or (3) nonadhesive (n = 5, n = 3, and n = 1, respectively). MRI images (T2) were used to evaluate the presence of peritumoral CSF as described in an MRI-based method of assessing adhesions.[32]

Tumor adherence grade was evaluated perioperatively with a three-level scale. Four tumors were described as nonadhesive, three as partially adhesive, and two were completely adhesive. The agreement between perioperatively assessed adhesion and predicted adhesion was 89% (95% confidence interval [CI] 57%–98%). The agreement between CSF clefts and perioperative adhesion was 21%. The difference in SII and CSF cleft prediction was not significant. A trend with decreasing OSS values in completely adhesive tumors was observed.

The second study[33] included 25 patients with MENs ($\geq$2.5 cm in diameter). Patients underwent single frequency MRE (60 Hz) prior to surgical resection. OSS maps and shear line images were generated, in a similar manner to the previous study.[5] Normalized OSS maps were generated to assess how the wave amplitude affected the OSS prediction. Adhesion was classified as (1) complete (*low frequency shear line, or high OCC contour in >2/3 of the interface*), 2) partial (*–||– 1/3*), or (3) no slip interface. OSS maps and shear line images described 22 tumors as complete, one as partial, and two as having no slip interface. Normalized OSS maps described 15 as complete, 4 as partial, and 6 as having no slip interface.

The dissection plane was described during resection as (1) extrapial (nonadhesive and separated from the pial surface), (2) mixed (areas of adhesion, and areas of nonadhesion), or (3) subpial (adhesive, and resection was subpial in more than 2/3 of the interface) (n = 15, n = 4, and n = 6, respectively). The Cohen κ coefficient between surgical dissection plane and OSS/shear line maps was 0.37 (95% CI 0.05–0.69) indicating a fair agreement. The Cohen κ coefficient for surgical findings and normalized OSS maps was 0.86 (95% CI 0.69–1), indicating good agreement. The correlations between OSS maps, shear line results, and normalized OSS maps with surgical findings were significant ($P = 0.02$, $P = 0.02$, and $P < 0.0001$, respectively). The study indicates a possible role of SSI in predicting meningioma adhesion preoperatively, and normalization of the maps seems to improve the predictive ability.

DISCUSSION

Technical Challenges and Comments on Translation

A detailed technical discourse is beyond the scope of this review, but a few points are necessary to note.

MRE has several sources of errors, including longitudinal wave effect, simultaneous differences in shear wave speed, and prestress effects.[1] In addition, the inversion algorithms are based on several assumptions such as the lack of tissue boundaries and tissue homogeneity, so the in vivo conditions are not necessarily accurately reflected. A tissue border/edge bias has been described and occurs due to differences in tissue homogeneity at interfaces. This may again cause wave reflection, scattering, and interference.[34] Tissue geometry and inherent properties can affect wave behavior (waveguide effect).[1]

The resolution of elastographic details is limited. While MRE can measure tissue properties that vary by five orders of magnitude,[9] the actual level of detail that can be appreciated remains low as resolution remains a limiting factor. For example, Murphy et al[23] had to exclude a small meningioma because no pixels remained in the ROI. Other studies[25,27] excluded tumors with diameters of less than 2 cm. Hughes et al[25] reported that the lowest agreement was present in small soft tumors with a hard component. Brain MRE results are generally reproducible when the same method is applied, but caution is warranted when comparing results across studies.[35] Summarizing results across studies is difficult due to variations in acquisition parameters, post-processing, study design, cohorts, and units. For example, variations in driving frequencies display different regions of the non-linear stress/strain relationship in viscoelastic bodies. Other challenges related to soft tissue behavior are central; for details on soft tissue rheology and its implications for MRE, the reader is referred to Bilston's review on this topic.[13] Table 3 is an overview of tumor sizes and applied strategies for reducing edge biases.

Reporting viscoelastic parameter in a precise and standardized manner is essential when performing MRE studies. Unfortunately, the use of loosely defined terms and a variable level of detail in reporting of methodology makes accurate parameter identification challenging. For example, the parameter reported by Xu et al[16] is "elasticity" which they extract by local frequency estimation in which wave speed is extracted; assumedly this is then converted to

TABLE 3. Tumor Sizes and Edge Correction

Authors, Year	Tumor Sizes	Edge Effect?
Xu et al 2007	Max dia. range 38–75 mm	Not accounted for
Simon et al 2013	Improbable volumes reported	Curl of the wave field
Sakai et al 2016	Max dia. range 14–94 mm	Avoided interference fringes on wave images and cross hatches on G' maps.
Reiss-Zimmerman et al 2015	Vol. range 25–633 mm^3	MDEV inversion
Murphy et al 2013	One meningioma was excluded due to small size because no pixels remained after erosion	Removed edges of tumor mask by central and six connected pixel erosion. Curl of the wave field
Hughes et al 2015	Max dia. range 22–90 mm	Curl of the wave field
Streitberger et al 2014	Vol. range 5.9–140 mm^3	MDEV inversion
Pepin et al 2018	Vol. range 41–1170 mm^3	Curl of the wave field
Streitberger et al 2020	Vol. range 59–804 mm^3	MDEV inversion

dia. indicates diameter; MDEV, multi-frequency dual elasto-visco; vol., volume.

shear stiffness (U) by squaring wave speed and assuming density to be that of water thus U is reported. ''Stiffness'' is reported by several authors but refers to widely different parameters. In general stiffness refers to the real part of the complex modulus, that is, the storage modulus (G') in contrast to the loss modulus (G'').[1] This is believed to be the case in Murphy et al.[23] In Hughes et al,[4,25] because (1) they reported using a direct inversion algorithm from the curl of the data which would provide $G* = G' + iG''$, (2) other authors have concluded similarly.[36] However, they do define ''stiffness'' as wave speed squared which implies that shear stiffness (U) is actually the reported parameter. From our point of view additional background data is required to make a firm conclusion. Sakai et al[20] reports shear stiffness (U) but background data did not allow us to verify that this was the actual described parameter.

Discriminative Potential

Bunevicius et al[36] made a pooled data analysis of five studies comparing storage (G') and loss (G'') moduli and shear modulus phase angle (φ) 95% CI. Their analysis included results from Hughes et al,[4] Sakai et al,[20] Reiss-Zimmerman,[21] Simon et al,[18] and Streitberger et al.[26] GBMs (n = 39), MENs (n = 22), PMAs (n = 21), metastases (n = 8), AAs (n = 6), VS (n = 21), and low-grade gliomas (n = 5). Only low-grade gliomas compared to meningiomas using the loss modulus (G'') and shear modulus phase angle (φ) had nonoverlapping 95% CI. Three of the studies included NAWM ROIs, and a pooled analysis comparing $\Delta G'$, $\Delta G'$, and $\Delta\varphi$ in tumor/NAWM was made to reduce inter-study biases. In this analysis, meningiomas could be distinguished from gliomas and brain metastases by $\Delta\varphi$. No other tumors could be distinguished due to overlapping CIs. As the technical challenges are addressed, the discriminative ability of MRE may improve. For example, better resolution may visualize patterns of elastic changes intrinsic to the ECM and allow exploration of variations in tumor architecture. Viscoelastic models such as the springpot model are related to the fractal geometry of the tissue[13,37] and have been applied in brain MRE studies on dementias. In breast tumor studies, springpot power law coefficients and shear modulus increased with increasing malignancy.[7] These parameters remain to be applied in brain tumor studies.

Predicting Intraoperative Conditions

Studies assessing intraoperative tumor consistency, adhesion, and heterogeneity are of special interest due to the direct implications for tumor resectability and prognosis.[38] For example, soft meningiomas can be removed entirely by suction while hard meningiomas may require ultrasonic aspiration at high settings and piecemeal resection. The introduction of less invasive techniques such as endoscopic approaches augments the need for preoperative noninvasive acquisition of this information.

Two studies attempted to predict meningioma consistency. Murphy et al[23] correlated both storage moduli (G') and the ratio $G'_{\text{tumor}}/G'_{\text{peritumor}}$ with intraoperative consistency. The study has limited direct translational value, however, because the statistical analysis is rank-based. Future studies should for example apply ordinal regression models to define a mathematical function that models the relationship between the ranked surgical outcome and the MRE measured predictor. Murphy et al reported a single outlier, where the tumor was graded as 2/5 (i.e., mostly soft) while the mean G' of the tumor and peritumoral region was the highest in the cohort. The applied pixel inversion may have been biased towards the stiffest part of the tumor adjacent to the dura.[23] Notably, there was evidence of increased intracranial pressure (ICP) in this patient, and preloading may have shifted the stress/strain relationship.[1] A reduction of ICP during craniotomy may explain the low intraoperative consistency grade. Studies on how ICP affects measured values are limited (Table 4). Static preload causes overestimation of stiffness in liver MRE studies.[39] In large animal studies, a positive linear relationship between acute pressure changes and $|G*|$ was described.[40] A case report with low pressure hydrocephalus described reduced stiffness with an increase to normal levels following recovery/normalization of ICP.[41] Currently the bias may be reduced by calculating the stiffness ratio of tumor and NAWM, but the preload effect on brain and tumor tissue probably differs. Preoperative ICP measures may have a role in controlling for preload effects. A pilot study by Andersen et al[42] suggests a funduscopic approach for noninvasive ICP-measurements, but the method requires further inquiry. The effect of ICP on brain MRE measures should further be elucidated to allow for correction. These studies should consider regional variations in ICP and model preload effects with respect to tissue type.

Hughes et al[25] showed a significant correlation between intraoperative consistency and G'. While they used a similar 5-point scale for intraoperative assessment, they grouped rank 4 and 5 tumors as hard while rank 1–3 tumors were grouped as soft. The lowest agreement was found in small tumors that were predicted to be soft but intraoperatively were found to have a hard portion. The inaccuracy may be related to the limited spatial resolution of elastographic detail. Durometric measurements were applied to yield semi-quantitative assessments of consistency. While this agreed with both intraoperative and surgically assessed consistency, this approach has limitations. For reference measures, elastic tissue indentation techniques should be considered because they allow quantitative and reproducible mechanical assessments of tissue properties. For example, axial strain could be applied on surgical specimens at different

TABLE 4. MRE and ICP

Authors, Year	Results
Arani et al 2018[2] Large animal study	Large animals: positive correlation between $\|G*\|$ and ICP 90 Hz (0.017 ± 0.002 kPa/mmHg, $P = .001$) 120 Hz (0.030 ± 0.004 kPa/mmHg, $P < 0.0001$) 150 Hz (0.031 ± 0.008 kPa/mmHg, $P = 0.001$)
Olivero et al 2020[31]	At time of LPH 1.62 kPa (± 0.51 kPa)
Case report: Low pressure hydrocephalus (LPH)	At time of recovery 2.67 kPa (± 0.92 kPa)

MRE indicates magnetic resonance elastography.

loading velocities, thus evaluating strain-rate dependent stress/strain relationships. Several soft tissue indentation protocols have been described (Table 5). By limiting strain to 1% during indentation, the almost linear part of the stress/strain relationship in soft tissues may be sampled, thus mimicking the displacement common in MRE studies.[13] Slow loading velocities (0.01 mm/s) may simulate the stress/strain rates during surgical procedures,[43] but higher strain rates may better mimic palpation. An indentation depth of 10% reduces the effect of sample height and is believed to improve test reproducibility.[44] A probe with a diameter less than 25% of sample diameter should be applied.[45] Shear rheometry is another option and can be applied to introduce shear stress to tumor biopsies. These approaches would bridge MRE- and laboratory-based rheology and may provide valuable insights into both fields. Furthermore, these laboratory techniques may be modified and applied in an intraoperative setting and thus quantitatively supplement the current haptic consistency grading.

While Hughes et al performed well in correlating hardness and heterogeneity in meningiomas, the ability to rule in homogeneity and softness was lower. Standardized reproducible assessment of tumor heterogeneity is challenging. For example, Zada et al[3] reported a kappa score of 0.67 (95% CI 0.41–0.86) when two surgeons assessed meningiomas heterogeneity intraoperatively. In contrast, the consistency assessment had a kappa score of 0.87 (0.76–0.99). The surgeons may overestimate heterogeneity, consistency, etc when resecting tumors in difficult locations as technically challenging operations can be experienced as more demanding. This becomes especially relevant when comparing tumors in different regions. Future studies on tumor heterogeneity should consider these factors—for example, by registering 3D locations of inhomogeneous regions on neuronavigation platforms and defining separate ROIs corresponding to these regions on the following MRE analysis. Statistical analyses should control for regional variation. Although the brain shift phenomenon would affect the accuracy of the locational data, elastograms could be imported directly into neuronavigation platforms so that sites of inhomogeneity could be defined intraoperatively.

Sakai et al[20] and Hughes et al[4] compared PMA with intraoperative consistencies. Sakai et al used video recordings to assess how much suction, ultrasonic aspiration, etc was required for resection. Mean G' and G'_{max} correlated with a 2-grade consistency assessment (soft, hard). Hughes et al separated soft and intermediate consistency PMAs using G'. No hard tumors were included in the study. Both studies indicate that MRE contributes with information applicable in a clinical setting, but the study populations are small. Future studies should attempt to identify a cut-off point where transsphenoidal resection may no longer be preferred. This may reduce operation time and risk and improve preoperative planning.

Modeling Malignant Behavior

The invasive potential of tumors is closely related to tissue mechanics. MRE studies on glial tumors support a viscous fingering theory of invasive growth.[29] Viscous fingering is a fluid dynamic phenomenon that occurs due to the presence of interface instabilities under certain conditions. For example, the theory of Saffman-Taylor instabilities[46] demonstrates how a viscous driving fluid can displace a more viscous fluid by finger-like processes, the phenomena is known as Hele-Shaw flow (Fig. 3). The shear modulus phase angle (φ) measures a lag phase between compression and deformation and is therefore informative about the elasto-viscous duality (Table 1).[1] Reiss-Zimmerman et al[21] described an inverse relationship between φ and tumor grade. Only meningiomas had a $\varphi_{tumor}/\varphi_{NAWM}$ above one, while the $\varphi_{tumor}/\varphi_{NAWM}$ of the other (malignant) tumors were lower. Thus, malignant tumors were less viscous than normal parenchyma and—unlike meningiomas—meet the Saffman-Taylor conditions. Simon et al[18] described $\varphi_{tumor}/\varphi_{NAWM}$ below one in 7 out of 10 glial tumors. However, they used a lower driving frequency (45 Hz). In Streitberger et al,[26] 22 out of 22 GBM had lower φ than NAWM. In Streitberger et al,[28] GBM had lower φ than NAWM while meningiomas had higher φ than NAWM. In Bunevicius et al,[36] a pooled analysis revealed that the phase angle of meningiomas was significantly higher than that of malignant tumors (GBM, AA, low grade gliomas, and metastases). Only GBMs and metastatic tumors had mean φ with standard errors within the negative range, while meningiomas were clearly positive.

The studies by Streitberger et al, Reiss-Zimmerman et al, and Pepin et al all imply softer tumor consistency in higher grade tumors. This stands in contrast to tumors outside the central nervous system, where high stiffness is viewed as a trait of aggressive tumors.[47] The relative viscosity in combination with stiffness of malignant masses may therefore be informative in preoperative evaluation of aggressiveness

TABLE 5. Soft Tissue Indentation Studies

Authors, Year	Subject
Miller et al 1997[24]	Non-linear viscoelastic tissue model of porcine brain at different strain rates. Good agreement for strain reaching 30% compression.
Zheng et al 1999[45]	Compared ultrasound indentation with laboratory indentation of soft tissues using a linear assumption.
Gefen et al 2004.[13]	In vivo and in situ indentation of porcine brain.
van Dommelen et al 2010[47]	Compare average shear moduli at different strain rates of different brain regions in a bovine brain.
Griffin et al 2016[14]	Compression test on human cartilage by deriving Young's modulus from linear parts of the stress-strain curve
Forte et al 2016[11]	Deployed extensive mechanical testing including indentation on phantom materials to produce a composite hydrogel for brain tissue phantoms.
Stewart et al 2017[41]	Compared the steady state modulus of various brain tumors and surrogate material with a custom-built multiscale indenter.

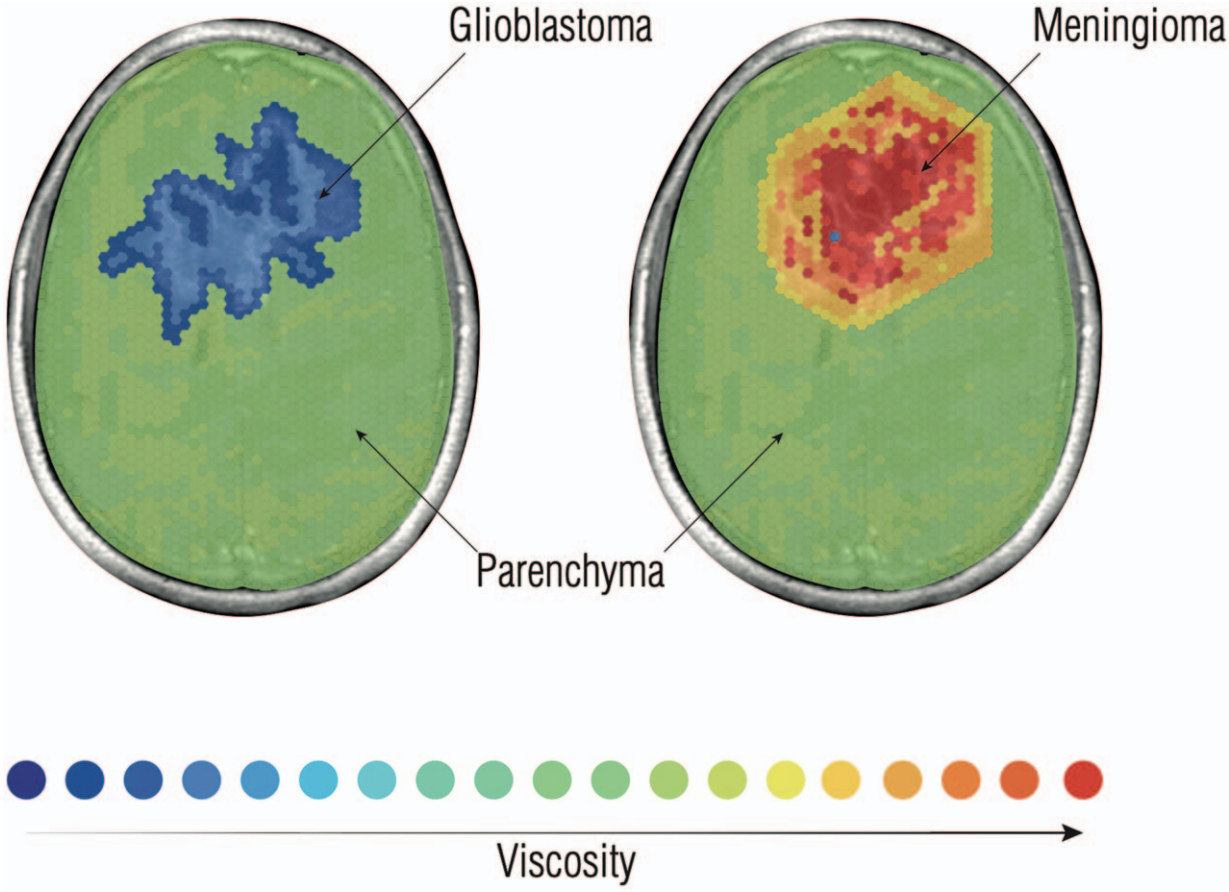

FIGURE 3. Hele-Shaw flow is the fluid dynamic observation that a viscous fluid may displace a more viscous fluid by the formation of finger like processes. This occurs due to interface instabilities (Saffman-Taylor instabilities). Similar models may contribute to our understanding of the growth patterns of malign neoplasm in the brain which is mostly fluid. MRE studies indicate that GBMs are less viscous than the brain parenchyma, and they grow by finger like processes. Meningiomas are generally more viscous than the brain parenchyma and grow expansively. GBM, glioblastoma; MRE, magnetic resonance elastography.

and may contribute to our understanding of the required conditions for invasive growth pattern. In line with this, glial tumor invasion seems to be related to viscoelastic differences in tumor and parenchyma (Fig. 3).

Genomechanics is an emerging field where tissue mechanical properties are explored in relation to genomic data. The study by Pepin et al[27] on IDH1-phenotypes demonstrated that wild type gliomas were softer than IDH1-mutated gliomas and found an inverse relationship between WHO grade and stiffness. Miroshnikova et al[6] described a correlation between glioma WHO grade, IDH mutation status, and ECM stiffness, measured with atomic force microscopy on biopsies.[6] ECM composition is a major contributor to the mechanical properties of tissues, and different ECM compositions may be reflected in MRE-derived parameters. Collagen content of tumor xenografts correlated positively with G' and G'' in animal studies and increased by similar quantities,[48] indicating that higher collagen content makes tumor stiffer ($G*$) by increasing both elastic and viscous components. This relationship may be descriptive for meningiomas, which have variable fibrous matrix fractions. As glial tumors have a high content of extremely hydrophilic GAGs, the matrix readily binds water in a gel-like substance[49] and remains more solid. Conversely, the ECM of meningiomas is rich in collagen and while still hydrophilic, is less so than GAGs. The high water content and fluid-like properties of meningiomas described by Streitberger et al, Simon et al, and Reiss-Zimmerman et al may indicate that the architecture resembles a porous network with fluid pockets. Fluidity translates to incompressibility and is thus reflective of the stiff haptic consistency that is frequently encountered. By comparing phase angle values and water content across a range of meningioma consistencies, this relationship can be explored further. The high phase angle values in meningiomas and the low phase angle values of gliomas may thus reflect the differences in ECM and interstitial composition. ECM stiffness has been demonstrated to directly affect glioma aggression,[6] and further insights may identify novel therapeutic targets. For example integrin is a promising therapeutic target due to its role in mechanotransduction and oncogenesis, the transmembrane receptor is widely expressed in both meningeal and glial tumors.[50]

Only Streitberger et al assessed the perifocal tumor region in their study on GBM, which was found to have similar stiffness $|G*|$, but increased φ when compared to NAWM. The microinvasive nature of glioblastomas renders diffuse borders that are poorly described on contrast-enhanced MRI. Future studies should explore the potential of detecting tumor nest and fingers in peritumoral regions. If detection of microinvasive tumor cells were improved, it could allow for

more aggressive resection in non-eloquent brain areas and may thereby improve prognoses.[51,52]

CONCLUSION

MRE studies on intracranial tumors are limited in number and highly heterogeneous in technical aspects and design. This reflects the novelty of a field which is rapidly advancing. MRE offers valuable insights into the mechanical physiology of intracranial tumors. Furthermore, MRE has several possible clinical applications that need to be further elucidated. Prediction of intraoperative consistency, adhesion, and tissue homogeneity seem particularly promising and MRE may have a role in staging and differentiating. Study samples are generally small, and comparison across studies is challenging and prone to bias. Inter-study biases can be reduced by more standardized image acquisition. Intra-study biases can be reduced by development and application of models correcting for preload effects, comparative measurements, and introduction of quantitative references. With increasing research, more standardized image acquisition, larger samples combined with technical advances improving resolution, and reflection of intraoperative conditions, MRE may prove to be a valuable paraclinical tool in a neurosurgical setting. MRE provides insight into in vivo mechanobiological conditions and widens our understanding of how structure is related to tumor behavior.

ACKNOWLEDGMENTS

We wish to thank MD-PhD Claire Gudex - medial writer, for contributing with proofreading and document editing.

Furthermore, we wish to thank Alioune Badara Diop and Ada arkitektur for his aid in graphical design.

REFERENCES

1. Manduca A, Bayly PJ, Ehman RL, et al. MR elastography: principles, guidelines, and terminology. *Magn Reson Med*. 2021;85:2377–2390.
2. Yao A, Pain M, Balchandani P, et al. Can MRI predict meningioma consistency? A correlation with tumor pathology and systematic review. *Neurosurg Rev*. 2018;41:745–753.
3. Zada G, Yashar P, Robison A, et al. A proposed grading system for standardizing tumor consistency of intracranial meningiomas. *Neurosurg Focus*. 2013;35:E1.
4. Hughes JD, Fattahi N, Van Gompel J, et al. Magnetic resonance elastography detects tumoral consistency in pituitary macroadenomas. *Pituitary*. 2016;19:286–292.
5. Yin Z, Glaser KJ, Manduca A, et al. Slip interface imaging predicts tumor-brain adhesion in vestibular schwannomas. *Radiology*. 2015;277:507–517. doi: 10.1148/radiol.2015151075.
6. Miroshnikova YA, Mouw JK, Barnes JM, et al. Tissue mechanics promote IDH1-dependent HIF1α–tenascin C feedback to regulate glioblastoma aggression. *Nat Cell Biol*. 2016;18:1336–1345.
7. Sinkus R, Siegmann K, Xydeas T, et al. MR elastography of breast lesions: understanding the solid/liquid duality can improve the specificity of contrast-enhanced MR mammography. *Magn Reson Med*. 2007;58:1135–1144.
8. Upadhyay N, Waldman AD. Conventional MRI evaluation of gliomas. *Br J Radiol*. 2011;84:S107–S111.
9. Mariappan YK, Glaser KJ, Ehman RL. Magnetic resonance elastography: a review. *Clin Anat*. 2010;23:497–511.
10. Muthupillai R, Lomas DJ, Rossman PJ, et al. Magnetic resonance elastography by direct visualization of propagating acoustic strain waves. *Science*. 1995;269:1854–1857.
11. Hiscox LV, Johnson CL, Barnhill E, et al. Magnetic resonance elastography (MRE) of the human brain: technique, findings and clinical applications. *Phys Med Biol*. 2016;61:R401–R437.
12. Yin Z, Romano AJ, Manduca A, et al. Stiffness and beyond: what MR elastography can tell us about brain structure and function under physiologic and pathologic conditions. *Top Magn Reson Imaging*. 2018;27:305–318.
13. Bilston LE. Soft tissue rheology and its implications for elastography: challenges and opportunities. *NMR Biomed*. 2018;31:e3832.
14. Muthupillai R, Ehman RL. Magnetic resonance elastography. *Nat Med*. 1996;2:601–603. doi: 10.1038/nm0596-601.
15. Tricco AC, Lillie E, Zarin W, et al. PRISMA Extension for Scoping Reviews (PRISMA-ScR): checklist and explanation. *Ann Intern Med*. 2018;169:467–473.
16. Xu L, Lin Y, Han JC, et al. Magnetic resonance elastography of brain tumors: preliminary results. *Acta Radiol*. 2007;48:327–330.
17. Xu L, Lin Y, Xi ZN, et al. Magnetic resonance elastography of the human brain: a preliminary study. *Acta Radiol*. 2007;48:112–115.
18. Simon M, Guo J, Papazoglou S, et al. Non-invasive characterization of intracranial tumors by magnetic resonance elastography. *New J Phys*. 2013;15:085024.
19. Sack I, Beierbach B, Wuerfel J, et al. The impact of aging and gender on brain viscoelasticity. *NeuroImage*. 2009;46:652–657.
20. Sakai N, Takehara Y, Yamashita S, et al. Shear stiffness of 4 common intracranial tumors measured using MR elastography: comparison with intraoperative consistency grading. *Am J Neuroradiol*. 2016;37:1851–1859.
21. Reiss-Zimmermann M, Streitberger KJ, Sack I, et al. High resolution imaging of viscoelastic properties of intracranial tumours by multi-frequency magnetic resonance elastography. *Clin Neuroradiol*. 2015;25:371–378.
22. Guo J, Hirsch S, Fehlner A, et al. Towards an elastographic atlas of brain anatomy. *PLoS ONE*. 2013;8:e71807.
23. Murphy MC, Huston J, Glaser KJ, et al. Preoperative assessment of meningioma stiffness using magnetic resonance elastography. *J Neurosurg*. 2013;118:643–648.
24. Oliphant TE, Manduca A, Ehman RL, et al. Complex-valued stiffness reconstruction for magnetic resonance elastography by algebraic inversion of the differential equation. *Magn Reson Med*. 2001;45:299–310.
25. Hughes JD, Fattahi N, Van Gompel J, et al. Higher-resolution magnetic resonance elastography in meningiomas to determine intratumoral consistency. *Neurosurgery*. 2015;77:653–658.
26. Streitberger KJ, Reiss-Zimmermann M, Freimann FB, et al. High-resolution mechanical imaging of glioblastoma by multifrequency magnetic resonance elastography. *PLoS ONE*. 2014;9:e110588.
27. Pepin KM, McGee KP, Arani A, et al. MR elastography analysis of glioma stiffness and IDH1-mutation status. *AJNR Am J Neuroradiol*. 2018;39:31–36.
28. Streitberger KJ, Lilaj L, Schrank F, et al. How tissue fluidity influences brain tumor progression. *Proc Natl Acad Sci U S A*. 2020;117:128–134.
29. Bogdan MJ, Savin T. Fingering instabilities in tissue invasion: an active fluid model. *R Soc Open Sci*. 2018;5:181579.
30. Chen Y-F, Fang S, Wu D-S, et al. Visualizing and quantifying the crossover from capillary fingering to viscous fingering in a rough fracture. *Water Resour Res*. 2017;53:7756–7772.
31. Mariappan YK, Glaser KJ, Manduca A, et al. Cyclic motion encoding for enhanced MR visualization of slip interfaces. *J Magn Reson Imaging*. 2009;30:855–863.
32. Yamada S, Taoka T, Nakagawa I, et al. A magnetic resonance imaging technique to evaluate tumor-brain adhesion in meningioma: brain-surface motion imaging. *World Neurosurg*. 2015;83:102–107.
33. Yin Z, Hughes JD, Trzasko JD, et al. Slip interface imaging based on MR-elastography preoperatively predicts meningioma-brain adhesion. *J Magn Reson Imaging*. 2017;46:1007–1016.
34. McGrath DM, Ravikumar N, Wilkinson ID, et al. Magnetic resonance elastography of the brain: an in silico study to determine the influence of cranial anatomy. *Magn Resonan Med*. 2016;76:645–662.

35. Svensson SF, De Arcos J, Darwish OI, et al. Robustness of MR elastography in the healthy brain: repeatability, reliability, and effect of different reconstruction methods. *J Magn Reson Imaging*. 2021;53:1510–1521.

36. Bunevicius A, Schregel K, Sinkus R, et al. REVIEW: MR elastography of brain tumors. *NeuroImage Clin*. 2020;25:102109.

37. Sack I, Jöhrens K, Würfel J, et al. Structure-sensitive elastography: on the viscoelastic powerlaw behavior of in vivo human tissue in health and disease. *Soft Matter*. 2013;9:5672–5680.

38. Stafford SL, Perry A, Suman VJ, et al. Primarily resected meningiomas: outcome and prognostic factors in 581 Mayo Clinic patients, 1978 through 1988. *Mayo Clin Proc*. 1998;73:936–942. doi: 10.4065/73.10.936.

39. Clarke EC, Cheng S, Green M, et al. Using static preload with magnetic resonance elastography to estimate large strain viscoelastic properties of bovine liver. *J Biomech*. 2011;44:2461–2465.

40. Arani A, Min H-K, Fattahi N, et al. Acute pressure changes in the brain are correlated with MR elastography stiffness measurements: initial feasibility in an in vivo large animal model. *Magn Reson Medicine*. 2018;79:1043–1051.

41. Olivero WC, Biswas A, Wszalek TM, et al. Brain stiffness following recovery in a patient with an episode of low-pressure hydrocephalus: case report. *Childs Nerv Syst*. 2020;37:2695–2698.

42. Andersen MS, Pedersen CB, Poulsen FR. A new novel method for assessing intracranial pressure using non-invasive fundus images: a pilot study. *Sci Rep*. 2020;10.

43. Miller K, Chinzei K. Constitutive modelling of brain tissue: Experiment and theory. *J Biomech*. 1997;30:1115–1121.

44. van Dommelen JA, van der Sande TP, Hrapko M, et al. Mechanical properties of brain tissue by indentation: interregional variation. *J Mech Behav Biomed Mater*. 2010;3:158–166.

45. Zheng Y, Mak AF, Lue B. Objective assessment of limb tissue elasticity: development of a manual indentation procedure. *J Rehabil Res Dev*. 1999;36:71–85.

46. Saffman PG, Taylor G. The penetration of a fluid into a porous medium or Hele-Shaw cell containing a more viscous liquid. *Proc R Soc Lond Ser A Math Phys Sci*. 1958;245:312–329.

47. Friedl P, Gilmour D. Collective cell migration in morphogenesis, regeneration and cancer. *Nat Rev Mol Cell Biol*. 2009;10:445–457.

48. Li J, Zormpas-Petridis K, Boult JKR, et al. Investigating the contribution of collagen to the tumor biomechanical phenotype with noninvasive magnetic resonance elastography. *Cancer Res*. 2019;79:5874–5883.

49. Bertolotto A, Giordana MT, Magrassi ML, et al. Glycosaminoglycans (GASs) in human cerebral tumors. *Acta Neuropathol*. 1982;58:115–119.

50. Huang J, Zhang L, Wan D, et al. Extracellular matrix and its therapeutic potential for cancer treatment. *Signal Transduct Target Ther*. 2021;6:153.

51. Chaichana KL, Cabrera-Aldana EE, Jusue-Torres I, et al. When gross total resection of a glioblastoma is possible, how much resection should be achieved? *World Neurosurg*. 2014;82:e257–e265.

52. Chaichana KL, Jusue-Torres I, Navarro-Ramirez R, et al. Establishing percent resection and residual volume thresholds affecting survival and recurrence for patients with newly diagnosed intracranial glioblastoma. *Neuro-Oncol*. 2014;16:113–122.